

Effect of HgI_2 intercalation on $\text{Bi}_2\text{Sr}_2\text{CaCu}_2\text{O}_y$: Interlayer coupling effect

Myoung-Kwang Bae, Mun-Seog Kim, and Sung-Ik Lee*

*Department of Physics, Pohang University of Science and Technology,
San 31 Hyojadong, Pohang, Kyungbuk, 790-784, Republic of Korea*

Nam-Gyu Park, Seong-Ju Hwang, Dong-Hoon Kim, and Jin-Ho Choy*

*Department of Chemistry, Center for Molecular Catalysis, College of Natural Sciences,
Seoul National University, Seoul 151-742, Republic of Korea*

(Received 10 November 1995)

By intercalating large HgI_2 molecules between the Bi_2O_2 layers in $\text{Bi}_2\text{Sr}_2\text{CaCu}_2\text{O}_y$, the distance between the CuO_2 blocks was significantly extended up to 7.2 \AA . The superconducting properties of this system were measured in various magnetic fields applied perpendicular to the CuO_2 planes. This system showed large positional fluctuation of the vortex even far below the transition temperature due to the reduction of dimensionality. The change of the thermodynamic parameters is well explained by the model of Josephson-coupled superconductivity. However, the interlayer coupling strength did not change the transition temperature drastically, which does not support the suggestion of Wheatley, Hsu, and Anderson of coherent hopping of the valence bond pair between the CuO_2 layers.

I. INTRODUCTION

Although it is well known that the superconductivity of cuprates is very much related to CuO_2 planes, details of the interlayer coupling effect are not well understood. Since the out-of-plane coherence length ξ_c at $T = 0 \text{ K}$ is smaller than the interlayer spacing, there is a dimensional crossover phenomena, where ξ_c is comparable to the interlayer distance.¹ The crossover temperature could depend on the interlayer coupling strength. Thus, if this coupling strength can be controlled, it will be very informative in understanding the relationship between interlayer coupling and superconductivity.

Recently, it was reported that a large molecule of HgX_2 ($X = \text{Br}, \text{I}$) could be intercalated between double Bi_2O_2 layers of high- T_c $\text{Bi}_2\text{Sr}_2\text{CaCu}_2\text{O}_y$ (Bi2212) superconductors.² According to magnetic susceptibility and powder x-ray diffraction measurements, it was found that the HgX_2 intercalation dropped T_c only by a small fraction even with the remarkable lattice expansion along the c axis ($\Delta \approx 7.2 \text{ \AA}$). Such results are different from those of iodine intercalation,^{3,4} with relatively larger T_c depressions and smaller lattice expansions. Therefore, since we can extend the distance between the CuO_2 blocks by the HgX_2 intercalation, this system would be an excellent example of obtaining the relationship between interblock coupling and superconductivity.

For the case of iodine intercalation, many efforts have been made to explain the effect of intercalation on superconductivity.³⁻⁷ Actually, superconductivity can be affected by the interlayer Josephson coupling due to the change of the interlayer distance of the CuO_2 layer and/or the modification of the electronic structure of the CuO_2 layer. However, instead of Josephson coupling, Wheatley, Hsu, and Anderson⁸ (WHA) accepted the coherent hopping of valence bond pairs between CuO_2 planes. The phase coherence between valence bonds is achieved by pairing the holons. But the applicability of this model to the intercala-

tion compounds has not yet been confirmed because an argument on two possible effects of intercalation, hole doping and the weakening of interblock coupling on the T_c depression, has remained unresolved for the case of iodine intercalation.³⁻⁷

In this paper, we have prepared grain-aligned $(\text{HgI}_2)_{0.5}\text{Bi}_2\text{Sr}_2\text{CaCu}_2\text{O}_y$ (HgI_2 -Bi2212) and measured its magnetization in various magnetic fields applied along the c axis, and compared it with that of pristine Bi2212. Since HgI_2 intercalation results in a remarkable lattice expansion, it is expected that the dimensionality of the system could be reduced and the thermodynamic parameters, such as the penetration depth and the Ginzburg-Landau parameter, will be significantly modified.

As expected, a reduction of the interlayer coupling strength and vastly enhanced positional fluctuation of the vortex were observed in the magnetization. The measured thermodynamic parameters are well explained by the change of the distance between superconducting CuO_2 layers,^{9,10} but the change of T_c is too small to support the coherent hopping of the valence bond pair suggested by Wheatley, Hsu, and Anderson.⁸

II. EXPERIMENT

An HgI_2 -Bi2212 compound was prepared by vapor transport reaction between the HgI_2 molecule and the pristine Bi2212. The polycrystalline Bi2212 pellet and mercuric iodine (mole ratio of 1:5), together with free iodine [$P(\text{I}_2) \approx 1.5 \text{ atm}$] as a transporting agent, were heated in an evacuated Pyrex tube. Details of the sample preparation were given in the previous report.² Formation of the HgI_2 intercalate and its stoichiometry were confirmed by powder x-ray diffraction (XRD) and thermogravimetric analysis (TGA) using the DuPont 2000 Thermal Analysis Station and electron probe microanalysis (EPMA), respectively.

To clarify the intrinsic anisotropic thermodynamic param-

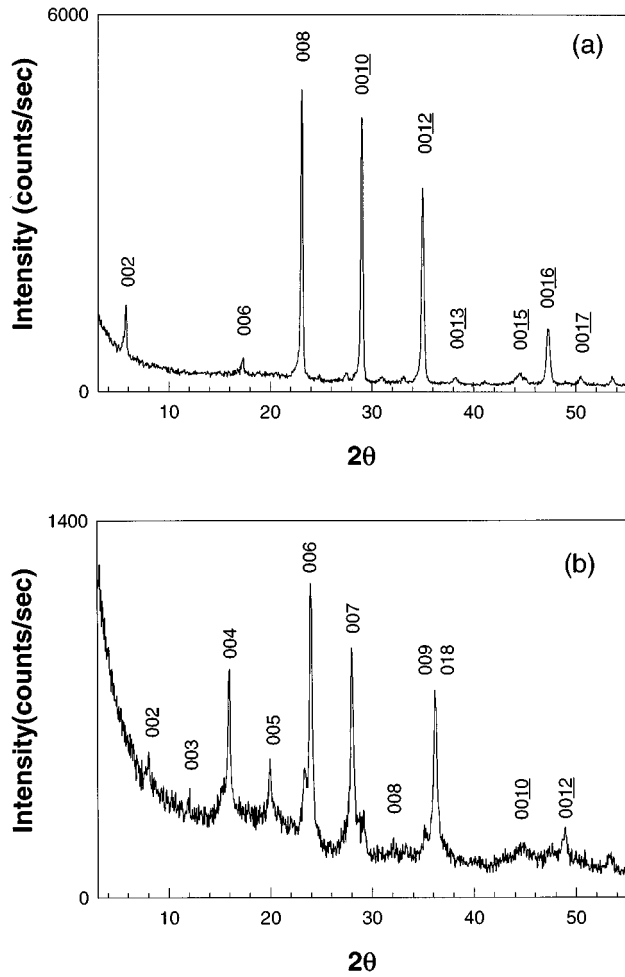


FIG. 1. X-ray powder diffraction patterns for the grain-aligned (a) pristine Bi₂Sr₂CaCu₂O_y and (b) its HgI₂ intercalate (HgI₂)_{0.5}Bi₂Sr₂CaCu₂O_y. The (00 l) reflections are predominant in XRD patterns, which confirms that each grain is well oriented along the c axis.

eters, Bi2212 and HgI₂-Bi2212 were ground down to less than 20 μ m, and were aligned simultaneously inside of the epoxy in a magnetic field of 7 T for 9 h. The resulting samples were examined by x-ray diffraction in Fig. 1. The (00 l) peaks predominant in the XRD data confirm that the grains are oriented with the c axis along the applied field.

The shielding [zero-field-cooled (ZFC)] and Meissner [field-cooled (FC)] magnetization at 10 G for these samples is shown in Fig. 2. The shielding values at 10 K were 67% for Bi2212 and 61% for HgI₂-Bi2212 without a demagnetization correction. The onsets of the superconducting transition for Bi2212 and HgI₂-Bi2212 were 85 K and 82 K, respectively. Both of these samples exhibited a very small step near 110 K due to the Bi₂Sr₂Ca₂Cu₃O_y phase with a volume fraction far less than 1%.

The magnetic measurements were performed in a Quantum Designs superconducting quantum interference device (SQUID) magnetometer for fields applied parallel to the c axis. Both background signals that originated from the epoxy and the holder were carefully subtracted.

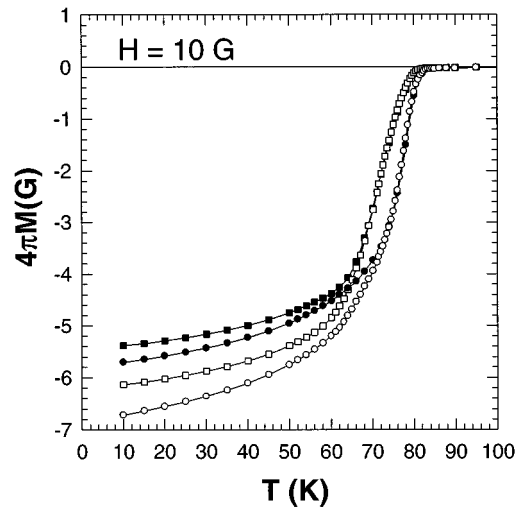


FIG. 2. The shield (ZFC, open symbols) and Meissner (FC, solid symbols) magnetizations of grain-aligned Bi₂Sr₂CaCu₂O_y (circle) and (HgI₂)_{0.5}Bi₂Sr₂CaCu₂O_y (squares) at $H=10$ G applied along the c axis.

III. RESULT AND DISCUSSION

According to XRD analysis, the c axis cell parameter of HgI₂-Bi2212 is 44.9 \AA , which corresponds to an increase of 14.3 \AA compared to that of pristine Bi2212. Since there are two intercalated layers of HgI₂ for each unit cell of Bi2212, the extent of lattice expansion per each intercalate layer corresponds to 7.2 \AA , which is almost twice that of the basal increment of iodine intercalation ($\Delta d=3.6$ \AA). Although mercuric iodide intercalation remarkably expands the c axis in Bi2212, it has little effect on the in-plane a and b parameters.

The XRD, after the grain alignment, experiment confirmed that the polycrystalline intercalate was well developed along the (00 l) planes (Fig. 1). Based on the observed (00 l) XRD patterns, a one-dimensional Fourier map from the structure factors $F_{(00l)}$ was calculated. As can be seen in Fig.

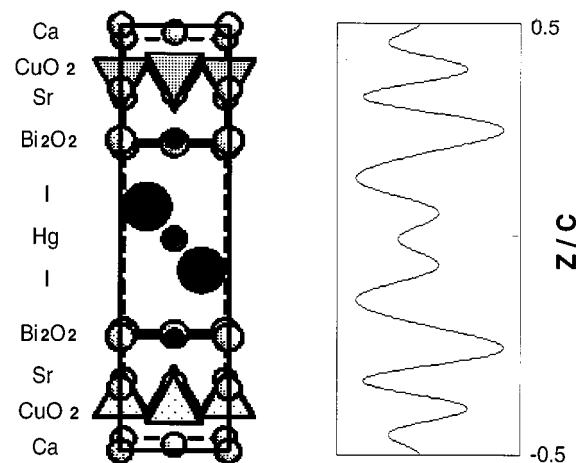


FIG. 3. Schematic structural model for grain-aligned HgI₂-intercalated Bi₂Sr₂CaCu₂O_y along with the one-dimensional Fourier map, which is based on the best fit to the observed XRD patterns.

TABLE I. Observed and calculated weight percents of each element in HgI_2 -intercalated $\text{Bi}_2\text{Sr}_2\text{CaCu}_2\text{O}_y$.

Elements	Observed value	Calculated value
Hg	9.10	9.18
I	12.80	11.60
Bi	38.13	38.28
Sr	11.17	12.04
Ca	5.66	5.51
Cu	11.32	11.64
O	11.82	11.73

3, the one-dimensional Fourier map clearly shows that the mercuric iodide molecule is intercalated in between the Bi_2O_2 double layer and the HgI_2 molecular axis is tilted with an angle of 48° with respect to the c axis. Based upon the electron density map, the schematic structure is represented (Fig. 3).

Figure 4 demonstrates the TGA curve of the HgI_2 intercalated sample for the temperature range between 20 and 800°C . The total weight loss at 800°C is 21.2%, which is in agreement with the calculated value of total loss of $(\text{HgI}_2)_{0.5}\text{Bi}_2\text{Sr}_2\text{CaCu}_2\text{O}_y$ (20.8%). EPMA also confirms the portion of HgI_2 in the sample. The average atomic ratio between Hg, I, and Bi was estimated to be 0.5:1:2, as summarized in Table I.

This chemically well-defined sample is used for the comparative study on the magnetization of Bi2212 and HgI_2 -Bi2212. For the detailed analysis, the vortex fluctuation model of Bulaevskii, Ledvij, and Kogan¹¹ (BLK) and the Hao-Clem model^{12,13} have been used. In the vortex fluctuation model, positional fluctuation of vortices, i.e., thermal distortion of two-dimensional pancake vortices out of the straight stacks near T_c , is considered. In the model of Hao and Clem, the free energy of the normal cores is also included but the effect of positional fluctuations is not. Thus, this model is valid at a temperature somewhat lower than T_c , where the vortex fluctuation is not dominant. Both theories are valid at the limited range of temperature. A proper

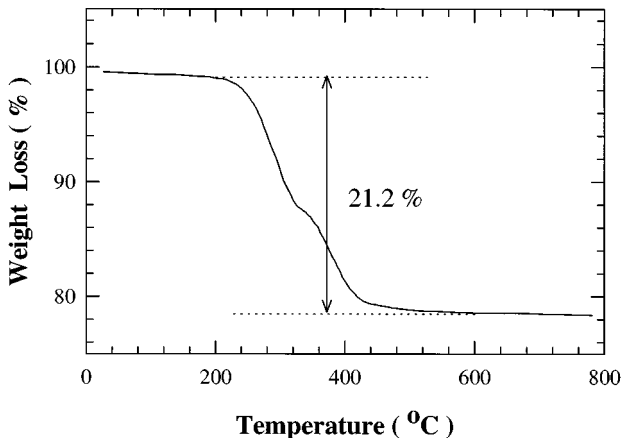


FIG. 4. Thermogravimetric curves for HgI_2 -intercalated $\text{Bi}_2\text{Sr}_2\text{CaCu}_2\text{O}_y$. Sample is heated under ambient atmosphere with a heating rate of $10^\circ\text{C}/\text{min}$.

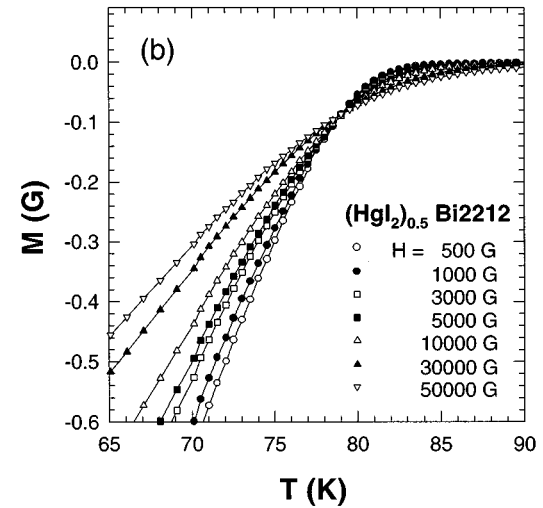
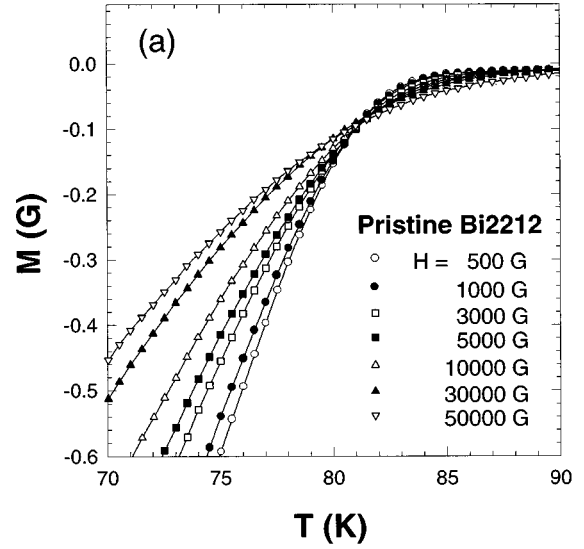


FIG. 5. The magnetizations of (a) $\text{Bi}_2\text{Sr}_2\text{CaCu}_2\text{O}_y$ ($M^* = -0.099 \pm 0.009$ G at $T^* = 80.7 \pm 0.25$ K) and (b) $(\text{HgI}_2)_{0.5}\text{Bi}_2\text{Sr}_2\text{CaCu}_2\text{O}_y$ ($M^* = -0.083 \pm 0.005$ G at $T^* = 79.2 \pm 0.25$ K) for $500 \text{ G} \leq H \leq 50\,000 \text{ G}$ applied perpendicular to the CuO_2 planes.

temperature range was chosen for the analysis.

BLK (Ref. 11) calculated the free energy of a mixed state in the frame of the Lawrence-Doniach model using a harmonic approximation. For the anisotropic ratio $\gamma \gg 1$ ($\gamma^2 = m_c/m_{ab}$ is the superpair effective mass ratio), for the applied magnetic field H parallel to c axis, and $B_{\text{cr}} \approx \phi_0/s^2\gamma^2 \ll H \ll H_{c2}$, they obtained the magnetization from the free energy, which includes the extra contribution of entropy due to thermally distorted pancakes,

$$-M(T, H) = \frac{\phi_0}{32\pi^2\lambda_{ab}^2} \ln \frac{\eta H_{c2}}{eH} - \frac{k_B T}{\phi_0 s} \ln \frac{16\pi k_B T \kappa^2}{\alpha \phi_0 s H \sqrt{e}}, \quad (1)$$

where $e = 2.718 \dots$, $\eta = 1.4$ (Refs. 12–14), s is the distance between superconducting layers, and α is a constant of order unity. The first term of Eq. (1) is London's result for unperturbed straight vortices and the second term originates

from the positional fluctuation of vortices. From Eq. (1) the slope $\partial M/\partial \ln H$ is easily calculated,

$$\begin{aligned} \frac{\partial M}{\partial \ln H} &= \frac{\phi_0}{32\pi^2\lambda_{ab}^2(T)} - \frac{k_B T}{\phi_0 s} \\ &= \frac{\phi_0}{32\pi^2\lambda_{ab}^2(T)} - \frac{|M^*|}{\ln(\eta\alpha/\sqrt{e})} \frac{T}{T^*}, \end{aligned} \quad (2)$$

where M^* is the magnetization value independent of the applied field, or $\partial M/\partial \ln H=0$ at T^* ,

$$-M^* \equiv -M^*(T^*) = \frac{k_B T^*}{\phi_0 s} \ln \frac{\eta\alpha}{\sqrt{e}}. \quad (3)$$

s is the distance between centers of two adjacent CuO₂ blocks. From the XRD analysis, s is found to be 15.3 Å for pristine Bi2212 and 22.5 Å for HgI₂-Bi2212.⁵ For the large anisotropic cuprate, it is reasonable to take $\ln(\eta\alpha/\sqrt{e})=1$.¹⁵

Figure 5 displays the magnetization of Bi2212 and HgI₂-Bi2212 for fields up to 5 T along the c axis. Both materials exhibit the field-independent magnetization M^* predicted by BLK. For pristine Bi2212, $M^* = -0.099 \pm 0.009$ G occurs at $T^* = 80.7 \pm 0.3$ K, and for HgI₂-Bi2212, $M^* = -0.083 \pm 0.005$ G at $T^* = 79.2 \pm 0.3$ K. Using isothermal magnetizations for $0.3 \leq H \leq 5$ T in the reversible region, we evaluate the experimental slopes $\partial M/\partial \ln H$ vs T and determine $\lambda_{ab}(T)$ using Eq. (2) (Refs. 14,16) (Fig. 6).

Hao and Clem's original idea is to use a variational method to minimize the Ginzburg-Landau free energy of the mixed state for a high- κ type-II superconductor.^{12,13} In this free energy, the $|\psi|^4$ is included. In the calculation, they also take into account the depression of the order parameter in the vortex cores. However, this model does not include the thermodynamic fluctuation in the magnetic fields and is not valid near T_c . The temperature dependence of κ and H_c can be evaluated using this model in reversible magnetization. The detailed description of this approach has been given in Refs. 13, 17. In summary, the general equation (4) of Ref. 17 was utilized to fit the reversible magnetization data at each temperature, where the fitting parameters are κ and critical fields $H_c(T)$. The experimental value of κ is determined to give the smallest deviation of $H_c(T)$. And the penetration depth $\lambda_{ab}(T)$ and coherence length $\xi_{ab}(T)$ could be extracted from κ and $H_c(T)$. The effect of the superconducting volume fraction from the magnetic susceptibility at 10 G is included in this analysis by dividing experimental magnetizations with the superconducting volume fraction.

In Fig. 6 the square symbols exhibit the result of a vortex fluctuation analysis. Solid lines are from the BCS temperature dependence of $\lambda_{ab}(T)$ deduced from the relations $H_{c2}(T) = \sqrt{2}\kappa H_c(T)$, $\sqrt{2}H_c = \kappa\phi_0/2\pi\lambda^2$, and the temperature dependence of $H_c(T)$,^{12,13}

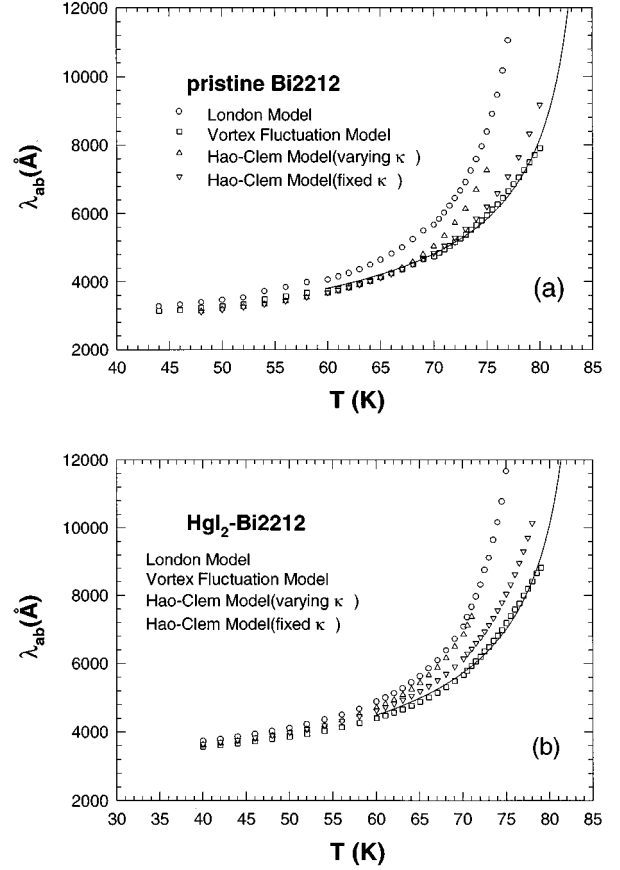


FIG. 6. In-plane penetration depth calculated with London model (circles), vortex fluctuation model (squares), and Hao-Clem model (triangles), considering a superconducting volume fraction. (a) Bi₂Sr₂CaCu₂O_y, (b) (HgI₂)_{0.5}Bi₂Sr₂CaCu₂O_y. Solid lines are fitted curves of the BCS expression.

$$\begin{aligned} \frac{H_c(T)}{H_c(0)} &= 1.7369 \left[1 - \frac{T}{T_c} \right] \left[1 - 0.2730 \left(1 - \frac{T}{T_c} \right) \right. \\ &\quad \left. - 0.0949 \left(1 - \frac{T}{T_c} \right)^2 \right] \quad (0.7T_c \leq T \leq T_c). \end{aligned} \quad (4)$$

The derived value of $\lambda_{ab}(0)$ from the above formula is 2599 Å with $T_c = 85$ K for Bi2212 and 3046 Å with $T_c = 84.5$ K for HgI₂-Bi2212. The circles indicate the $\lambda_{ab}(T)$ calculated from the London model. The unphysical divergence of the penetration depth below T_c for the London model and Hao-Clem model originates from ignorance of the positional fluctuation of vortices as indicated by Kogan *et al.*^{14,18–21} The values of λ_{ab} are not much different from those of the vortex fluctuation model at low temperature.

It is quite interesting to observe the positional fluctuation of the vortices from the calculated κ from the Hao-Clem model where this effect is not considered.^{12,13,17} The appearance of unphysical parameters such as λ_{ab} , κ could be evidence of the positional fluctuation of the vortices that is ignored in this fitting. In addition to the temperature-independent κ used in the Hao-Clem model, κ was also taken as a fitting parameter because κ usually decreases as

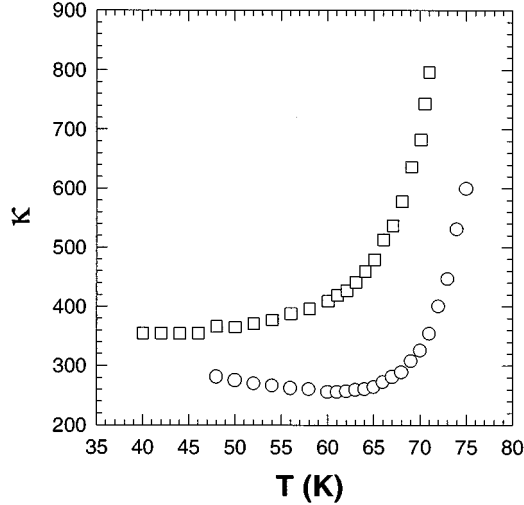


FIG. 7. Temperature dependence of κ of grain-aligned $\text{Bi}_2\text{Sr}_2\text{CaCu}_2\text{O}_y$ (circles) and $(\text{HgI}_2)_{0.5}\text{Bi}_2\text{Sr}_2\text{CaCu}_2\text{O}_y$ (squares).

temperature increases for type-II superconductors.²² The κ of Bi2212 (Fig. 7) shows the typical behavior of type-II superconductors for $T \leq 60$ K. The change of slope and subsequent divergence of κ above 65 K are artificial and are explained by neglecting the positional fluctuation as indicated at λ_{ab} .

What is the HgI_2 intercalation effect on κ ? Again, the same Hao-Clem model was used with κ as a fitting parameter. It is worthwhile to note the change of the slope $d\kappa/dT$ from negative to positive after intercalation for temperatures below 60 K. The positive $d\kappa/dT$ for HgI_2 -Bi2212 should be negative, if properly analyzed from the correct theory which includes both the positional fluctuation and vortex core contribution. The effect of the large size HgI_2 molecules, which reduce the dimensionality of the system drastically by increasing the distance between the CuO_2 blocks, enhances the two-dimensional vortex fluctuation effect down to 40° below T_c . In fact, the omission of the vortex fluctuation in the Hao-Clem model could be a useful tool, in reverse, to detect the development of vortex fluctuation for low-dimensional superconductors.

Then what are the correct thermodynamic parameters? The appropriate temperature range should be chosen for the analysis. Fortunately, as seen in Fig. 6, the values of λ_{ab} of Bi2212 from the Hao-Clem model are almost the same as those of the vortex fluctuation model at temperature ranges below 70 K. Since vortex fluctuation is strong at temperatures above 70 K, each analysis at the appropriate temperature range could give the right thermodynamic parameters of Bi2212. However, the situation is not simple for HgI_2 -Bi2212. The theory of Hao and Clem, which is valid at low-temperature ranges, is screened by an unusually strong vortex fluctuation. The combined theory which contains both the vortex fluctuation and the free energy contributions of the vortex core is needed.

For the thermodynamic parameters at $T=0$, we used the results of the Hao-Clem model and the two-fluid formula $H_c(T) = H_c(0)[1 - (T/T_c)^2]$. From this, we obtained $H_c(0) = 9753$ (8501) G with $T_c = 82.2$ (83.2) K for Bi2212 (HgI_2 -Bi2212). The formulas $H_{c2}(T) = \phi_0/2\pi\xi_{ab}^2$

TABLE II. Thermodynamic parameters of $\text{Bi}_2\text{Sr}_2\text{CaCu}_2\text{O}_y$ and $(\text{HgI}_2)_{0.5}\text{Bi}_2\text{Sr}_2\text{CaCu}_2\text{O}_y$.

Properties	$\text{Bi}_2\text{Sr}_2\text{CaCu}_2\text{O}_y$	$(\text{HgI}_2)_{0.5}\text{Bi}_2\text{Sr}_2\text{CaCu}_2\text{O}_y$
$s(\text{\AA})^a$	15.3	22.5
$T_{c,\text{onset}}$ (K)	85	82
M^* (G)	-0.099 ± 0.009	-0.083 ± 0.005
T^* (K)	80.7 ± 0.25	79.2 ± 0.25
	vortex fluctuation ^b	
$\lambda_{ab}(0)$ (\AA)	2599	3046
T_c (K)	85	84.5
	Hao-Clem model ^c	
κ^d	265.6 ± 8.8	371.9 ± 18.7
$H_c(0)$ (G)	9753	8501
T_c (K)	82.2	83.2
$\lambda_{ab}(0)$ (\AA)	2438	3197
ξ_{ab} (\AA)	9.5	8.6

^a s is obtained from an XRD analysis.

^b $\lambda_{ab}(0)$ and T_c are obtained from fitting the BCS formula to calculated $\lambda_{ab}(T)$.

^c $H_c(0)$ and T_c are obtained from a two-fluid fitting to the calculated $H_c(T)$.

^d κ is the averaged value obtained from the Hao-Clem analysis for $48 \leq T \leq 60$.

$= \sqrt{2}\kappa H_c(T)$ and $\sqrt{2}H_c = \kappa\phi_0/2\pi\lambda^2$ were used to obtain $\xi_{ab}(0) = 9.5$ \AA , $\lambda_{ab}(0) = 2438$ \AA for Bi2212, $\xi_{ab}(0) = 8.6$ \AA , $\lambda_{ab}(0) = 3197$ \AA for HgI_2 -Bi2212. These T_c values are slightly less than those obtained by utilizing the BLK theory and the T_c obtained by applying theories differs from the $T_{c,\text{onset}}$ measured from the 10 G magnetization. These differences of T_c originate from the different model fittings and different temperature ranges where the model is valid. This is within the error bar range of the analysis and was reported before for Bi2212 single crystals^{11,23} and other compounds^{17,20,24} (Table II).

Our $\lambda_{ab}(0)$ value of 2500 \AA is larger than the reported values of 1500 – 2150 \AA .^{11,25–27} This may come from the different oxygen contents; i.e., the oxygen contents of ours are not optimized for the highest superconducting transition temperature compared to the published samples. Due to this, our Bi2212 might be underdoped and its $\lambda_{ab}(0)$ larger than that of the literature as easily seen from Eq. (5) in the following paragraph.

One important result that must be explained is the ratio of $\lambda_{ab}(0)$ of 1.24 for HgI_2 -Bi2212 to that of the pristine sample. This ratio could be explained with the Josephson-coupled theory of superconductivity based on the Lawrence-Doniach model by Clem.^{9,10} In this theory,

$$\lambda_{ab} = \sqrt{\frac{m_{ab}^* c}{4\pi n_s e^{*2} s}} l, \quad (5)$$

where s is the thickness of the Josephson-coupled superconducting layer and l is the length of the stacking periodicity. If m_{ab}^* and n_s are almost the same before and after the intercalation of inert HgI_2 molecules, then the ratio of 1.24 is sim-

ply explained by the effect of the Josephson coupling strength change due to the 47% increase of the space between CuO₂ blocks.

Now we examine the applicability of the model of Wheatley, Hsu, and Anderson (WHA) to the intercalation compound. According to the WHA model, the superconducting transition temperature of Bi2212 superconductors can be expressed as⁸

$$T_c = \lambda_0 + \lambda_1,$$

where λ_0 is the interlayer coupling between the nearest planes (intrablock coupling) and λ_1 is interlayer coupling between the next-nearest planes (interblock coupling).

While HgI₂ intercalation has little effect on the intrablock coupling, the strength of the interblock coupling is remarkably reduced compared to the case of I₂ intercalation. Considering the larger lattice expansion of 7.2 Å for the HgI₂ intercalate, it is reasonably expected that HgI₂ intercalation further reduces the interblock coupling with respect to I₂ intercalation of the 3.6 Å expansion. In this respect, the T_c depression upon HgI₂ intercalation is suggested to be more prominent than that upon iodine intercalation. But the observed T_c depression for the HgI₂ intercalate is even smaller than that for iodine intercalation, which suggests that the coherence hopping of the valence bond pair between CuO₂ layers (WHA model) is not a unique mechanism for the intercalation compounds.

We found that the enhanced positional fluctuation of vortices and the change of the thermodynamic parameters after the intercalation of the inert molecule HgI₂ are mainly due to

the reduction of the Josephson coupling originating from the increase of the distance between the CuO₂ blocks. However, the interblock coupling is not critical for the change of the transition temperature.

IV. CONCLUSION

The superconducting properties of HgI₂-intercalated Bi2212 were studied. Several thermodynamic parameters were obtained by comparing the theories suggested by Bulaevskii *et al.* and Hao *et al.* The enhanced effect of fluctuation and the change of the thermodynamic parameters after intercalation of HgI₂ were successfully explained. Moreover, it was found that HgI₂ intercalation rarely affects the superconducting transition temperature of Bi2212 while it drastically increases the *c*-axis parameters. The reduction of the interlayer coupling strength explained the observed thermodynamic properties, but was not consistent with the coherent hopping of the valence bond pair between the CuO₂ superconducting layers suggested by Wheatley, Hsu, and Anderson.

ACKNOWLEDGMENTS

We wish to express appreciation for the financial support of the Korean Ministry of Education, Basic Science Research Centers of Pohang University of Science and Technology, Agency of Defense Development of Korea, Korea Science and Engineering Foundation, and the Korea Ministry of Science and Technology for the high- T_c superconductivity research.

* Authors to whom correspondence should be addressed.

¹S. L. Cooper and K. E. Grey, in *Physical Properties of High Temperature Superconductors*, edited by D. Ginsberg (World Scientific, Singapore, 1994), Vol. IV, p. 61.

²J. H. Choy *et al.*, *J. Am. Chem. Soc.* **116**, 11 564 (1994).

³X. D. Xiang *et al.*, *Nature* **348**, 145 (1990).

⁴X. D. Xiang *et al.*, *Science* **254**, 1487 (1991).

⁵J. H. Choy *et al.*, *J. Solid State Chem.* **102**, 284 (1993).

⁶D. Pooke *et al.*, *Physica C* **198**, 349 (1992).

⁷J. Ma *et al.*, *Physica C* **227**, 371 (1994).

⁸J. M. Wheatley, T. C. Hsu, and P. W. Anderson, *Nature* **333**, 121 (1988).

⁹J. R. Clem, *Phys. Rev. B* **43**, 7837 (1991).

¹⁰J. R. Clem, *Physica C* **162-164**, 1137 (1989).

¹¹L. N. Bulaevskii, M. Ledvij, and V. G. Kogan, *Phys. Rev. Lett.* **68**, 3773 (1992).

¹²Z. Hao and J. R. Clem, *Phys. Rev. Lett.* **67**, 2371 (1991).

¹³Z. Hao *et al.*, *Phys. Rev. B* **43**, 2844 (1991).

¹⁴V. G. Kogan *et al.*, *Phys. Rev. Lett.* **70**, 1870 (1993).

¹⁵Z. Tešanović *et al.*, *Phys. Rev. Lett.* **69**, 3563 (1992).

¹⁶M. K. Bae *et al.*, *Physica C* **228**, 195 (1994).

¹⁷M. S. Kim, M. K. Bae, W. C. Lee, and S. I. Lee, *Phys. Rev. B* **51**, 3261 (1995).

¹⁸Q. Li *et al.*, *Physica B* **194-196**, 1501 (1994).

¹⁹Q. Li *et al.*, *Phys. Rev. B* **46**, 3195 (1992).

²⁰Q. Li, M. Suenaga, T. Kimura, and K. Kishio, *Phys. Rev. B* **47**, 2854 (1993).

²¹D. N. Zheng, A. M. Campbell, and R. S. Liu, *Phys. Rev. B* **48**, 6519 (1993).

²²A. L. Fetter and P. C. Hohenberg, in *Superconductivity*, edited by R. Parks (Dekker, New York, 1969), p. 817.

²³J. C. Martínez *et al.*, *Phys. Rev. Lett.* **69**, 2276 (1992).

²⁴J. R. Thompson *et al.*, *Phys. Rev. B* **48**, 14 031 (1993).

²⁵L. Zhang, J. Liu, and R. N. Shelton, *Phys. Rev. B* **45**, 4978 (1992).

²⁶G. Triscone *et al.*, *Physica C* **224**, 263 (1994).

²⁷A. Schilling, R. Jin, J. D. Guo, and H. R. Ott, *Physica B* **194-196**, 2185 (1994).